BOREAS An international journal of Quaternary research

Multiple indicators record human adaptations to climatic change during the Middle Holocene at the Wanbei site in the middle and lower Huai River valley, China

WEIXIN TIAN, WUHONG LUO, HUIYUAN GAN, LIUGEN LIN, TIANCI SUN, YAJIE SUN, HANLIN XU, CAIWEI ZHANG, XIN WANG AND JUZHONG ZHANG

BOREAS

Tian, W., Luo, W., Gan, H., Lin, L., Sun, T., Sun, Y., Xu, H., Zhang, C., Wang, X. & Zhang, J.: Multiple indicators record human adaptations to climatic change during the Middle Holocene at the Wanbei site in the middle and lower Huai River valley, China. *Boreas*. https://doi.org/10.1111/bor.70010. ISSN 0300-9483.

The archaeological sediment successions from the Wanbei site provide an ideal case for reconstructing both natural and human-induced environmental changes in the middle and lower reaches of the Huai River valley located in the transitional zone of eastern China during the Middle Holocene. The findings of this work, in terms of phytoliths, pollen and spores, and chemical elemental analyses suggest that the climatic conditions that were recorded in the Wanbei profile responded well to broader climatic changes, with an overall warm and humid climate during 5700–5300 a BP, albeit with a cooling trend between 5600 and 5400 a BP. Rice (*Oryza sativa*) was always the main cereal crop in mixed rice-millet farming owing to warm and humid conditions, although the proportions of broomcorn millet (*Panicum miliaceum*) and foxtail millet (*Setaria italica*) significantly increased during the cooling period. The structural characteristics and adjustments of mixed farming over time show an adaptation strategy in response to the climatic changes at Wanbei. Furthermore, multiple indicators reveal that human activities at the Wanbei site would increase rather than decrease during the cooling period between 5600 and 5400 a BP. This study not only highlights the dynamic nature of early agricultural societies, but also enhances our understanding of their adaptation strategies in response to climatic changes in the middle and lower Huai River valley during the Middle Holocene.

Weixin Tian, Wuhong Luo (corresponding author: lwh0551@ustc.edu.cn), Tianci Sun, Yajie Sun, Hanlin Xu, Caiwei Zhang, Xin Wang and Juzhong Zhang, Department for the History of Scientific Archaeology, University of Science and Technology of China, Hefei 230026, China; Huiyuan Gan, Institute of Archaeology, Nanjing Museum, Nanjing 210016, China; Liugen Lin, School of Art and Archabology, Zhejiang University, Hangzhou 310058, China; *received 14th August 2024, accepted 2nd April 2025.*

Human activities and climate change have an interdependent relationship, which has significant social and economic implications and has attracted increasing attention in the research community in recent decades (Chen *et al*. 2015; Cruz *et al*. 2017; Park *et al*. 2019; Perşoiu *et al*. 2019; Ran & Chen 2019; Pleskot *et al*. 2020). Many lines of evidence illustrate that social development, especially in prehistoric times, was highly vulnerable to climatic changes (Dong *et al*. 2012; Kajita *et al*. 2018; Murari *et al*. 2018; Kawahata 2019; Jia *et al*. 2021). Moreover, human activities, especially agriculture, have significantly affected the structure, processes and functions of ecosystems during the Holocene (Sun *et al*. 2021; Zapolska *et al*. 2023). Understanding past human–climate interactions has important implications both for exploring the long-term developmental process of human culture and agriculture and for better assessing human adaptation strategies in the context of longer-term climatic changes (Dearing *et al*. 2006; Burdanowitz *et al*. 2019).

The middle and lower Huai River valley, located in the transitional region between the northern subtropical and warm temperate zones, as well as the humid and semihumid zones in eastern China, are sensitive to both global and regional climatic change. Since the Early Holocene, the region has experienced frequent human activities and finally became an important part of the birthplace of Chinese civilization (Zhou 1999; Zhang 2018). Hence, the distinctive geographical and cultural characteristics of the middle and lower Huai River valley make it an ideal region for studying the relationships between human activities and climatic changes.

Over recent decades, multi-proxy analyses of natural sediments (e.g. pollen, spores, foraminifera; Jin *et al*. 1987; Tang *et al*. 1993) have not only reconstructed Holocene climate evolution sequences but also substantiated the pivotal role of climatic changes in driving the evolution of human subsistence strategies in this region (Hu *et al*. 2018; Jiang *et al*. 2018; Yu *et al*. 2024). Those studies, however, were unable to establish a high-resolution chronology for the association of climatic changes and human activities, because the analysed natural deposits (i.e. lacustrine sediments and peat layers) are commonly discontinuous and cover long time spans. Additionally, archaeological sedimentary records based on phytolith analysis at the Shuanshanji site (Wu *et al*. 2017; Luo *et al*. 2021), magnetic susceptibility and elemental geochemistry analysis at Yuchisi and Yuhuicun sites (Ma *et al*. 2006; Xu 2009; Zhang *et al*. 2010) and pollen and spores analysis at Wanbei site (Tang *et al*. 1991) focussed mainly on climatic changes and their interactions with ancient culture during the existence of each site. Despite

DOI 10.1111/bor.70010

intensive palaeoclimate research and associated archaeological studies over the last decades, the climatic conditions and how ancient humans adapted to the changes during the Neolithic Age are still poorly understood, especially during the critical period of the emergence of social complexity in the middle and lower Huai River valley.

The Wanbei site (34°15′22.3″ N, 118°49′57.6″ E), located approximately 15 km north of Shuyang County, Jiangsu Province, lies at the intersection of the Yi River and Shu River, which are two tributaries of the Huai River (Fig. 1). Multiple excavations reveal that the site has local characteristics and is significantly influenced by Haidai cultures, as seen in the unearthed objects that cover the Beixing Culture, Dawenkou Culture, Yueshi Culture and others (Nanjing Museum 1992), which were key time points in the emergence of social complexity and the origin of Chinese civilization. Previous studies have indicated that mixed farming of rice and millet (Cheng *et al.* 2020; Tian *et al.* 2023) and animal husbandry (Li 1991), together with gathering, hunting and fishing, were significant subsistence strategies and that slight climatic fluctuations occurred during the prehistoric period (Tang *et al.* 1991). However, the relationships among climate change, cultural exchanges and agriculture at the site are ignored.

Indeed, the particle distributions at archaeological sites are governed by both natural deposits and inputs from human activities (Wallis 2001). Many significant advances in reconstructing regional climatic changes and human activities from archaeological sediment successions have demonstrated that it is crucial to extract and interpret the main influences of human activity and environmental change separately. Therefore, archaeological sediment successions are considered one of the best archives that can provide information on the relationships among climate and human activities, although some controversies still exist regarding the reconstruction of palaeoenvironments (Huang & Zhang 2000; Li *et al.* 2008, 2010; Xiao *et al.* 2011; Qiu *et al.* 2014). In this study, multiple indicators, including analyses of phytoliths, pollen, chemical elements and microcharcoal, are investigated to describe human activities and regional climatic changes and to explore their relationships at the Wanbei site. This study provides a window into a better understanding of adaptation strategies in response to climatic changes during the Holocene.

Material and methods

Stratigraphy and sampling

Wanbei site lies on an elevated plateau to the NW of Gushuoxiang Lake. This area is typically dominated by the East Asian monsoon, with an average annual temperature of 13.8°C and an average annual precipitation of 937.5 mm (Ge *et al.* 2008). The vegetation in the Wanbei region consists of warm temperate deciduous broad-leaved forests dominated by *Quercus variabilis*, *Quercus acutissima*, *Pinus densiflora* and others. A test trench (T1) with surface dimensions 10 × 10 m, located to the SE of the Wanbei site, was excavated in 2015.

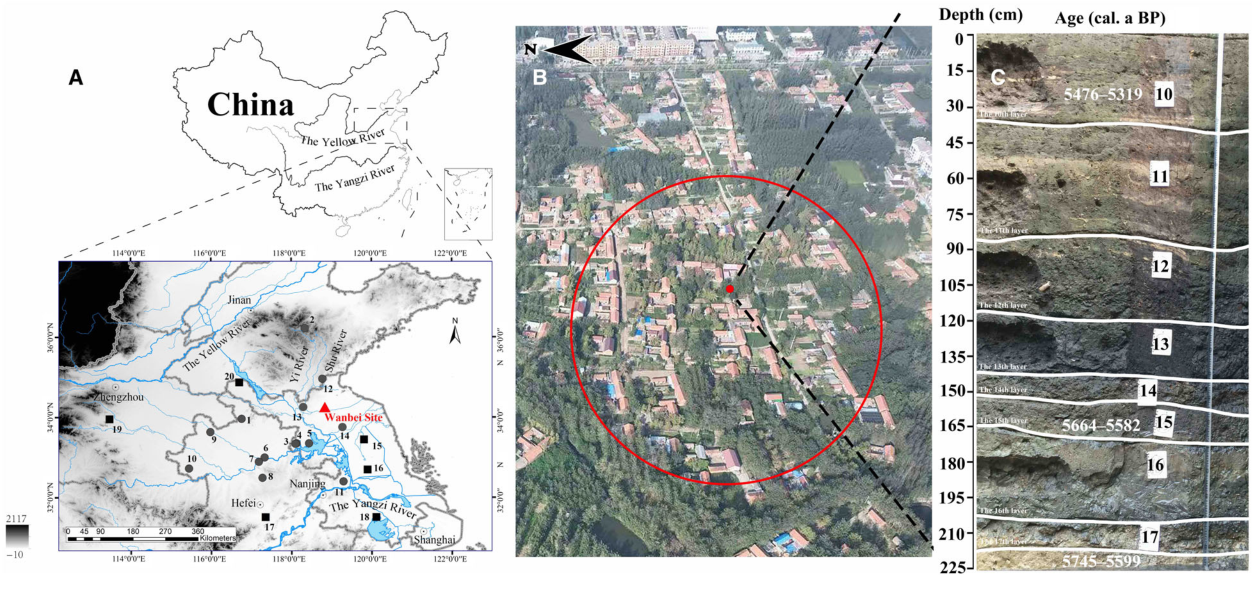

Fig. 1. A. Map showing the location of the Wanbei site and other sites mentioned in the article. 1, Qugou site; 2, Bianbiandong site; 3, Shunshanji site; 4, Hanjing site; 5, Xuenan site; 6, Shuangdun site; 7, Yuhuicun site; 8, Houjiazhai site; 9, Houtieying site; 10, Gongzhuang site; 11, Longqiuzhuang site; 12, Dongpan site; 13, Huating site; 14, Qingliangang site; 15, Qingfeng profile; 16, Zhouzhuang profile; 17, Chaohu lake core; 18, Guxv lake core; 19, Xiangcheng profile; 20, Huangkou core. B. The red circle indicates the scope of the Wanbei site and the red dot indicates the location of trail trench (T1). C. The sampled profile in the south wall of trail trench (T1) with stratigraphy and calibrated AMS ^{14}C ages at the Wanbei site.

Table 1. Description of the stratigraphy, south wall of trail trench (T1) at the Wanbei site.

Layer	Depth (cm) below ground surface	Lithology	Sedimentary faces
10	0–40	Grey clay containing sand and gravel, red-fired particles and charcoal fragments	Cultural layer
11	40–90	Brown clay containing charcoal fragments	Cultural layer
12	90–120	Black soil containing shells and animal bones	Cultural layer
13	120–150	Black soil containing pottery artefacts	Cultural layer
14	150–160	Grey clay containing bone remains and charcoal fragments	Cultural layer
15	160–170	Black clay containing coarse sand, charcoal fragments, bones and pottery	Cultural layer
16	170–200	Grey clay containing charcoal fragments	Cultural layer
17	200–210	Grey clay containing charcoal fragments	Cultural layer
18	210–225	Grey clay	Natural layer

Table 2. AMS ^{14}C dating obtained from the T1 profile at the Wanbei site (Tian *et al.* 2023).

Layer	Laboratory code	Dated material	^{14}C age (a BP)	Calibrated age (2σ) (cal. BC)	Median calibrated age (cal. a BP)
10	28444	Charred *Trapa*	4680±30	3526–3369 (95.4%)	5476–5319
11	28445	Charred *Trapa*	4420±30	3322–3237 (14.9%) 3177–3160 (1.8%) 3106–2921 (78.7%)	5056–4871
14	28446	Charred *Trapa*	4960±30	3795–3649 (95.4%)	5745–5599
15	25028	Charcoal	4890±30	3763–3737 (3.8%) 3714–3632 (91.7%)	5664–5582
18	25029	Charcoal	4960±30	3795–3649 (95.4%)	5745–5599

The south wall of T1, with a depth of 225 cm, is divided into nine lithological layers, ranging from layer 10 to layer 18 from top to bottom, according to the stratigraphy, soil colour and archaeological remains (Fig. 1; Table 1). A total of five chronological data points have been reported previously for the profile at the Wanbei site (Tian *et al.* 2023), indicating that the ages of the sediment samples range from ~5700 to ~5300 a BP (Table 2). On the basis of the linear relationship between date and depth, approximate age ranges were calculated for each layer. A total of 30 soil samples were taken successively from this profile at intervals of approximately 5 cm and were sampled for phytolith, pollen, microcharcoal and chemical element analyses in this study.

Analyses

Phytolith analysis. – In total, 30 samples were selected for phytolith analyses. Phytoliths were extracted from the soil samples according to the procedures outlined by Piperno (2014) and Luo *et al.* (2019). Firstly, each soil sample (~5 g) was placed in a 500 mL beaker, and 500 mL of 5% SHMP (sodium hexametaphosphate) solution was added and stirred for deflocculation. Secondly, the samples were treated with 30% hydrogen peroxide (H_2O_2) and cold 10% hydrochloric acid (HCl) to remove organic matter and carbonates, and a *Lycopodium* spore tablet (10 315 grains per tablet) was then added to each sample. Thirdly, the phytoliths were separated using zinc bromide ($ZnBr_2$, density 2.35 g cm^{-3}) as a heavy liquid and then rinsed with 95% ethanol until the supernatants were clear. The phytolith residues were mounted in silicon oil and scanned under a Leica DM 4500P microscope at 400–630× magnification. Nearly 500 phytoliths were counted in each sample, fast scanning of the slide was then conducted to identify the main phytolith morphotypes of the cereal crops and *lycopodium* spores were added to calculate their concentrations. The identification and classification of phytoliths were aided by published references and criteria (Wang & Lu 1993; Lu *et al.* 2009; Ball *et al.* 2016; Zhang *et al.* 2018), and their designations were issued in accordance with the International Code for Phytolith Nomenclature 2.0 (ICPN 2.0) (International Committee for Phytolith Taxonomy 2019).

Pollen and microcharcoal analysis. – In total, 30 samples were selected for pollen and microcharcoal analyses. Pollen and microcharcoal extractions were conducted on the soil samples based on the procedure described by (Faegri *et al.* 1989) with slight modifications, and a *Lycopodium* spore tablet was added to each sample as a tracer. In brief, each soil sample (~40 g) was placed into four 50 mL centrifuge tubes, and the preparation procedures then involved the removal of carbonates using 18% HCl and siliceous materials using 45% hydrofluoric acid (HF). The pollen and microcharcoal were concentrated by heavy-liquid flotation with $ZnBr_2$ (density of 2.0 g cm^{-3}) to separate them from the undigested minerals. The pollen and microcharcoal samples were counted via a Leica DM4500P optical microscope. Pollen identification was aided by an illustrated guide to modern pollen and spores (Wang *et al*. 1996; Song *et al*. 1999). Moreover, Poaceae pollen grains were divided into two categories on the basis of diameter and size (long axis): ≥38 and <38 μm. Then, fast scanning was also conducted to detect the coarse microcharcoal (≥50 μm), and lycopodium spores were added to calculate their concentrations in each sample.

Chemical elements analysis. – A total of 15 samples were selected for elemental determinations of the ALS minerals through spaced sampling. After the samples were air dried, 2 g of each sample was placed in an agate mortar and ground to a size finer than 200 mesh. Perchloric acid ($HClO_4$), nitric acid (HNO_3), HF and HCl were separately used for digestion, and diluted HCl was then used to determine the volume. Finally, inductively coupled plasma emission spectroscopy was used for the analyses.

Results

All AMS ^{14}C dating results in this study fell within the range of 5740–5319 calibrated years BP (68.3%), although the dates from layers 11 and 14 exhibit minor deviations potentially attributable to post-depositional disturbances. Integrating these radiocarbon dates with the stratigraphic succession of the Wanbei site, the selected cultural layers 18–11 correspond to the early Dawenkou culture period, while cultural layer 10 represents the middle Dawenkou culture period. By integrating the relative chronological succession of artefact types with the absolute dating results, we established a reliable chronological framework for the Wanbei site profile. Furthermore, the stratigraphic profile has been divided into five distinct zones based on fluctuations in microfossil assemblages. These zones have been corroborated by the CONISS results in TG View 2.0 software (Grimm 1987). Zone I includes layer 17 and layer 16; Zone II includes layer 15 and layer 14; Zone III includes layer 13 and layer 12; Zone IV includes layer 11; and Zone V includes layer 10.

Phytolith analysis results

More than 20 well-preserved phytolith types were recovered from most samples at the site. The identified crop phytoliths include BULLIFORM and BILOBATE with scooped ends parallel arrangement from *Oryza sativa*, DOUBLE PEAKED from rice husks, η-type from inflorescence bracts of *Panicum miliaceum*, Ω-type from inflorescence bracts of *Setaria italic*. The other phytoliths consist of CUNEIFORM BULLIFORM, BILOBATE, BLOCKY, RECTANGLE, SMOOTH-ELONGATE, ELONGATE-ECHINATE, siliceous vessel, SHORT SADDLE, LONG SADDLE, WAVY TRAPEZOID, ACICULAR, RONDEL, β-type from husks of barnyard grass (*Echinochloa* spp.) and POLYHEDRONS with conical projection. SCUTIFORM BULLIFORM was from reeds (*Phragmites* spp.) and other microfossil remains (e.g. sponge spicules, diatoms and charcoal) (Fig. 2).

According to the classification of Wang & Lu (1993), warm-type grasses can produce CUNEIFORM BULLIFORM, BILOBATE and SHORT SADDLE, whereas cold-type grasses mainly produce RONDEL, WAVY TRAPEZOID, SMOOTH-ELONGATE, ELONGATE-ECHINATE and ACICULAR. The *Iw* is a ratio of the number of warm types (including BULLIFORM, SADDLE, BILOBATE) to the total number of warm and cold type (including RONDEL, WAVY TRAPEZOID, SMOOTH-ELONGATE, ELONGATE-ECHINATE and ACICULAR) phytoliths, with higher values corresponding to warmer temperatures (Wang *et al*. 2003):

$$Iw = \frac{\text{warm type}}{\text{warm type} + \text{cold type}} \quad (1)$$

Zone I (225–175 cm) is dominated by warm-type phytoliths, which include mainly BILOBATE (9.29%), RECTANGLE (5.93%), SHORT SADDLE (5.80%), CUNEIFORM BULLIFORM (5.29%) and BLOCKY (1.33%). RONDEL (9.47%), ELONGATE-ECHINATE (6.23%), SMOOTH-ELONGATE (4.79%) and WAVY TRAPEZOID (4.63%) occupy relatively lower proportions. The mean value of *Iw* is 0.60, ranging from 0.46 to 0.68. In total, 2427 phytoliths are counted from the samples, of which a total of 247 DOUBLE PEAKED from rice husks (for a ubiquity of 100%), 157 BULLIFORM from *O. sativa* (for a ubiquity of 100%), 21 BILOBATE with scooped-end parallel arrangements (for a ubiquity of 100%) and eight η-type from inflorescence bracts of *P. miliaceum* (for a ubiquity of 60%) are recovered. The estimated average concentrations of these phytoliths are 10 875.52, 6773.70, 865.19 and 350 grains g^{-1}, respectively (Fig. 3). The statistics for these crop seed phytoliths show that rice and broomcorn millet constitute 96.86% and 3.14% of the total crops, respectively (Fig. 4).

Zone II (175–150 cm) features a predominance of warm types. The BILOBATE, RECTANGLE, CUNEIFORM BULLIFORM, BLOCKY and SHORT SADDLE account for 10.79, 5.14, 2.33, 2.90 and 2.14%, respectively, whereas SMOOTH-ELONGATE, RONDEL, ELONGATE-ECHINATE and WAVY TRAPEZOID account for 9.12, 6.15, 6.36 and 2.42%, respectively. The mean value of *Iw* is 0.53, ranging from 0.46 to 0.61. A total of 2606 phytoliths are counted, of which 480 DOUBLE PEAKED from rice husks (for a ubiquity of 100%), 109 BULLFORM from *O. sativa* (for a ubiquity of 100%), 18 BILOBATE with scooped-end parallel arrangements (for a ubiquity of 100%), 1 Ω-type from inflorescence bracts of *S. italic* (for a ubiquity of 20%) and 80 η-type from inflorescence bracts of *P. miliaceum* (for a ubiquity of 100%) are recovered. The estimated average concentrations of these phytoliths were 15 399.35, 3219.57, 610.68, 45.84 and 2641.30 grains g^{-1}, respectively (Fig. 3). The statistics for

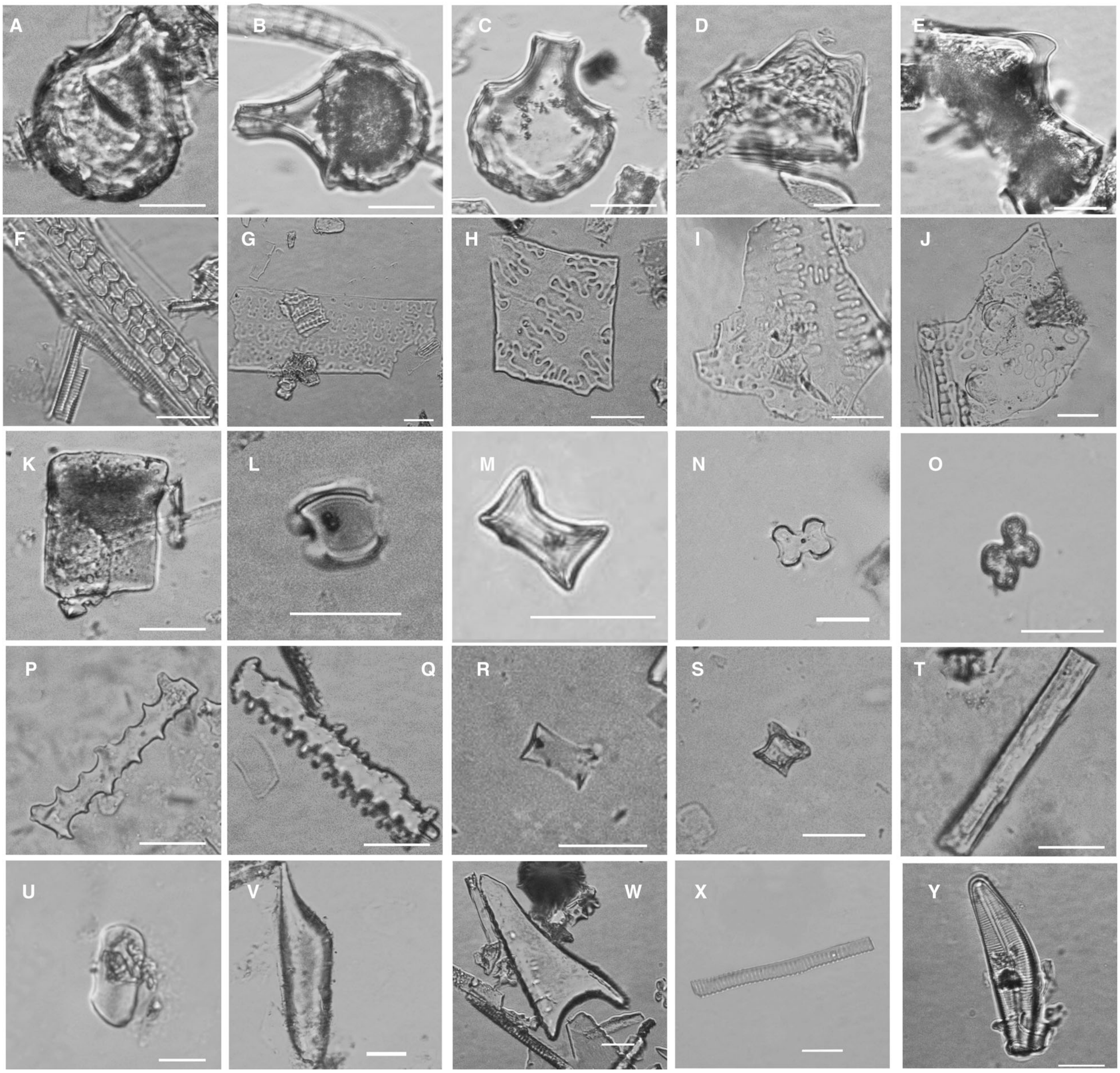

Fig. 2. Main phytoliths morphotypes and other microfossils found at the Wanbei site. A–C. BULLIFORM from *Oryza sativa*. D, E. DOUBLE PEAKED from *Oryza sativa*. F. BILOBATE with scooped ends paralleled arrangement from *Oryza sativa*. G–I. η-Type from inflorescence bracts of *Panicum miliaceum*. J. Ω-type from husks of *Setaria italica*. K. RECTANGLE. L. SHORT SADDLE. M. LONG SADDLE. N, O. BILOBATE. P, Q. ELONGATE-ECHINATE. R, S. RONDEL. T. SMOOTH-ELONGATE. U. WAVY TRAPEZOID. V, W. ACICULAR. X. vascular tissues. Y. Diatom. Scale bar: 20 μm.

these crop seed phytoliths show that rice, foxtail millet and broomcorn millet constitute 85.56, 1.78 and 14.26% of the total crops, respectively (Fig. 4).

Zone III (150–90 cm) is characterized by a slight increase in cold types. Elongate long cells (9.94%), elongate echinate cells (5.46%), rondle short cells (7.31%) and WAVY TRAPEZOID (2.67%) account for 25.38%, and BILOBATE (12.09%), CUNEIFORM BULLIFORM (2.08%), RECTANGLE (4.89%), BLOCKY (2.86%) and SHORT SADDLE (2.58%) account for 24.5%. The mean value of *Iw* is 0.49, ranging from 0.39 to 0.56. A total of 5392 phytoliths are counted in this zone, where 637 DOUBLE PEAKED from rice husks (for a ubiquity of 100.00%), 82 BULLIFORM from *O. sativa* (for a ubiquity of 100.00%), 48 BILOBATE with scooped-end parallel arrangements (for a ubiquity of 88.89%), two Ω-type from inflorescence bracts of *S. italic* (for a ubiquity of 22.23%) and 115 η-type from inflorescence bracts of *P. miliaceum* (for a ubiquity of 100%) are recovered. The estimated average concentrations of these phytoliths are 9489.47, 1720.07, 568.36, 25.92 and 2076.59 grains g^{-1}, respectively (Fig. 3). The statistics for these crop seed phytoliths show that rice, foxtail millet and broomcorn millet constitute 84.48, 2.65 and 15.25% of the total crops, respectively (Fig. 4).

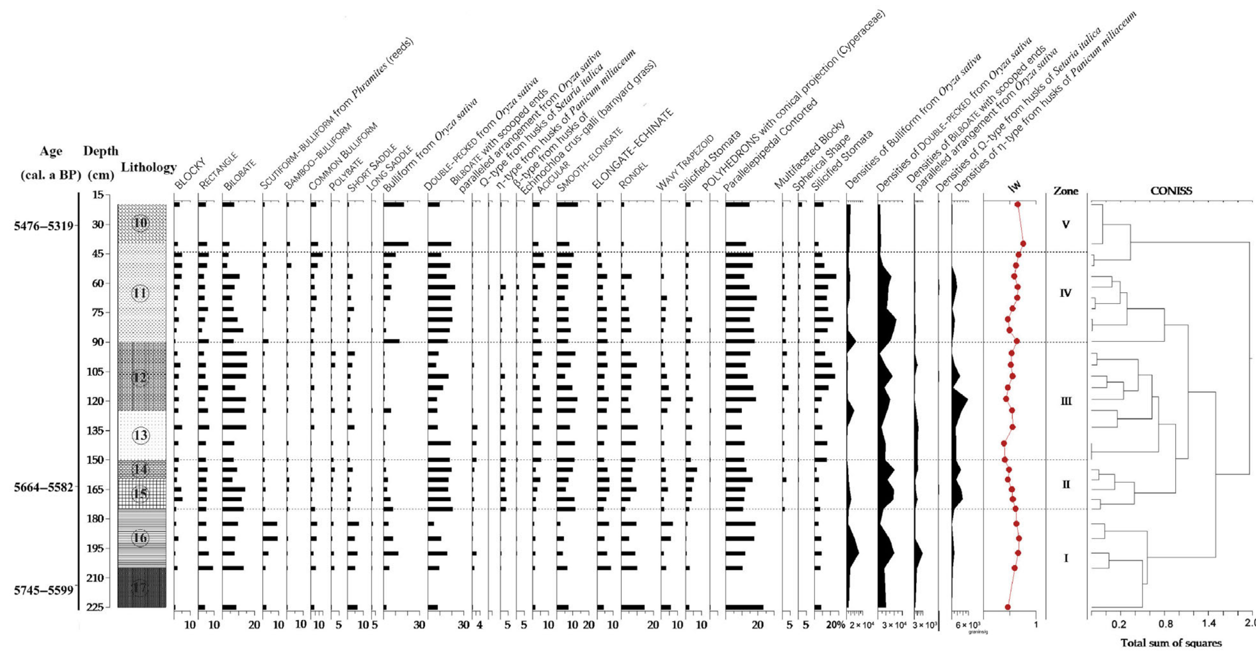

Fig. 3. Phytolith percentage diagram with selected morphotypes for the sampled T1 at the Wanbei site (modified after Tian *et al.* 2023). Lithological details are provided in Table 1.

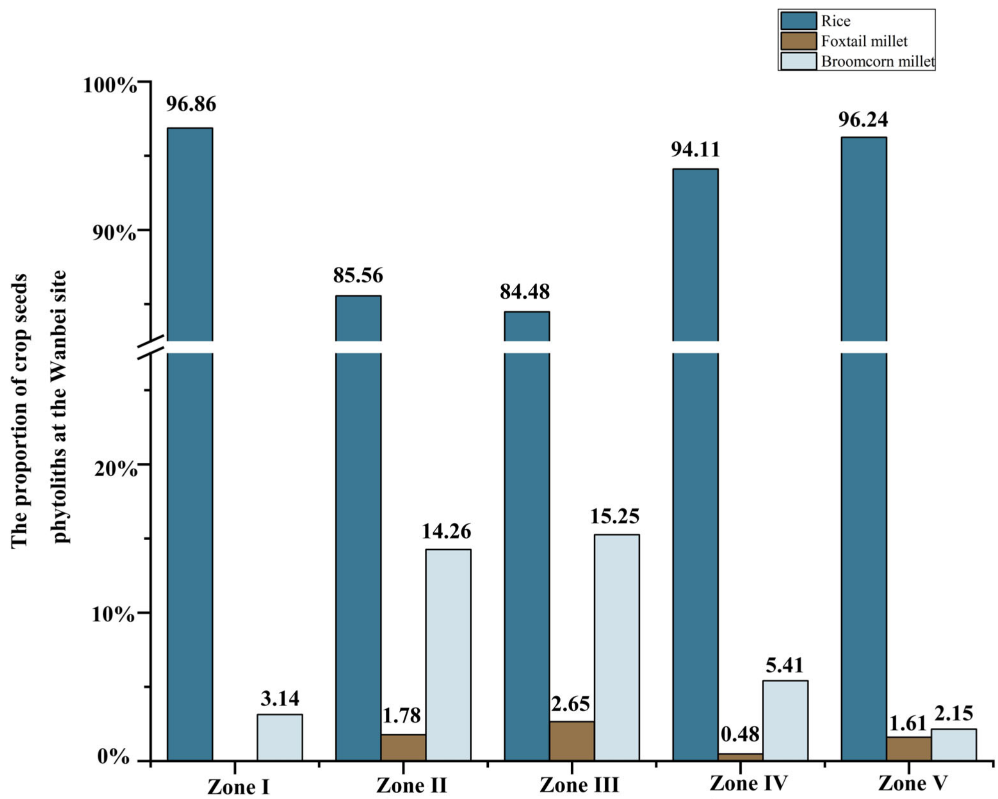

Fig. 4. The proportions of crop seeds phytoliths over time at the Wanbei site.

Zone IV (90–40 cm) indicates the flourishing of warm types. Bilobate, Cuneiform Bulliform, Rectangle, Blocky and Short Saddle account for 7.37, 5.54, 4.62, 2.92 and 1.82%, respectively. The main type of cold phytolith accounts for only 17.02% of the total. The mean value of *Iw* is 0.59, ranging from 0.46 to 0.67. In total, 5519 phytoliths were counted in this zone, in which a total of 990 Double Peaked from rice husks (for a ubiquity of 100.00%), 311 Bulliform from *O. sativa* (for a ubiquity of 100.00%), 11 Bilobate with scooped-end parallel arrangements (for a ubiquity of 100%), five Ω-type from inflorescence bracts of *S. italic* (for a ubiquity of 22.23%) and 57 *η*-type from inflorescence bracts of *P. miliaceum* (for a ubiquity of 77.78%) were recovered. The estimated average concentrations of these phytoliths were 13 065.77, 3532.40, 143.33, 50.27 and 762.84 grains g^{-1}, respectively (Fig. 3). The statistics for these crop seed phytoliths show that rice, foxtail millet and broomcorn millet represented 94.11, 0.48 and 5.41% of the total crops, respectively (Fig. 4).

Zone V (40–0 cm) is conspicuously marked by warm-growing types. The *Iw* values range from 0.65 to 0.76, and the mean value of *Iw* is 0.71. A total of 1229 phytoliths were counted in this zone, of which 179 Double Peaked from rice husks (for a ubiquity of 100%), 231 Bulliform from *O. sativa* (for a ubiquity of 100%), two Bilobate with scooped-end paralleled arrangements (for a ubiquity of 100%), three Ω-type from inflorescence bracts of *S. italic* (for a ubiquity of 100%) and four *η*-type from inflorescence bracts of *P. miliaceum* (for a ubiquity of 100%) were recovered. The estimated average concentrations of these phytoliths were 2914.71, 3945.35, 34.99, 56.04 and 77.09 grains g^{-1}, respectively (Fig. 3). The statistics for these crop seed phytoliths show that rice, foxtail millet and broomcorn millet represented 96.24, 1.61 and 2.15% of the total crops, respectively (Fig. 4).

Pollen and spore, and microcharcoal analysis results

A total of 39 pollen and spore types were identified, including 18 tree and shrub pollen types, 17 herbaceous pollen types and four fern spore types. The common types of tree and shrub pollen are mainly from Fagaceae, *Pinus*, evergreen *Quercus*, Betulaceae, *Carpinus*, *Juglans*, *Ulmus* and Moraceae. The herbaceous pollen types are characterized by Poaceae, *Artemisia*, Chenopodiaceae, Cruciferae, Labiatae, Caryophyllaceae and Gentianaceae, and hygrophyte pollen consists of Cyperaceae and Typhaceae (Fig. 5). The common spore types include *Concentricystes* and *Ceratopteris*. However, extremely low contents of pollen grains are observed in most samples at Wanbei. The data for the samples from the same layers are, therefore, combined with the statistics in this study.

Previous studies have revealed that the pollen particles of Poaceae crops generally become larger (≥38 μm) than those of wild Poaceae plants; therefore, they are often considered a symbol of agricultural activity, with their concentrations reaching a certain value (such as >15–20%) or higher (Li *et al*. 2012; Wang *et al*. 2017). Additionally, the microcharcoal concentrations from natural and archaeological sediments have been shown to vary in association with the strength of natural fires and human activities, respectively (MacDonald *et al*. 1991; Li *et al*. 2008; Shu *et al*. 2010). Hence, the changes in the proportions of Poaceae pollen ≥38 μm in size and the concentrations of coarse-grained microcharcoal, which are mainly found in their original positions, are adopted to reflect the development of agricultural activities and the intensity of human activities within the Wanbei archaeological site in this paper, respectively.

In Zone I, the pollen assemblages are predominantly characterized by herbaceous pollen, specifically Poaceae pollen, with relative abundances ranging from 30.36 to 41.92%. This is followed by Chenopodiaceae pollen, which accounts for 0.87–8.03% of the pollen. Arboreal pollen includes *Pinus* (3.93–8.93%), Fagaceae (3.06–3.57%), evergreen *Quercus* (1.31–1.78%) and Betulaceae (2.68%). Hygrophyte pollen is composed mainly of *Typha* (8.30–10.71%). Fern spores, particularly *Ceratopteris* spores, constitute a significant proportion, with relative abundances between 12.22 and 21.43%. The average total sum for herbaceous pollen is 55.12%, that of arboreal pollen is 15.47%, and that of fern spores is 28.75% (Fig. 6). The proportion of Poaceae pollen with a size ≥38 μm represents 33–44% of the total Poaceae pollen (Fig. 7). The mean concentration of coarse-grained microcharcoal is 14 533.83 grains g^{-1} (Fig. 7).

In Zone II, there was an increase in the percentage of herbaceous pollen, particularly Poaceae pollen, with relative abundances between 49.09 and 51.28%, and Chenopodiaceae pollen, which ranged from 5.98 to 12.12%. In contrast, *Pinus* pollen dramatically decreases to 0–5.8%, and arboreal pollen from evergreen *Quercus* and *Ulmus* nearly vanishes. Hygrophyte pollen, such as *Typha* (3.03–5.12%) and Cyperaceae (1.12–1.71%), as well as algae spores, such as *Ceratopteris* (3.42–4.84%), sharply decreased compared with Zone I. The average total sum of herbaceous pollen was 69.33%, that of arboreal pollen was 14.5%, and that of fern spores was 14.7% (Fig. 6). The proportions of herbaceous pollen increased, whereas the proportions of fern spores decreased notably. The proportions of Poaceae pollen with a size ≥38 μm account for 52.17–63.8% of the total Poaceae pollen (Fig. 7). The mean concentration of coarse-grained microcharcoal is 14 513.2 grains g^{-1} (Fig. 7).

In Zone III, the pollen assemblages are still dominated by Poaceae pollen, with relative abundances between 50.00 and 54.23%. Arboreal pollen is characterized primarily by Fagaceae (5.08%) and *Salix* (3.33%). Hygrophyte pollen consists mainly of Cyperaceae (3.33–4.23%) and *Typha* (3.33–6.80%). The average total

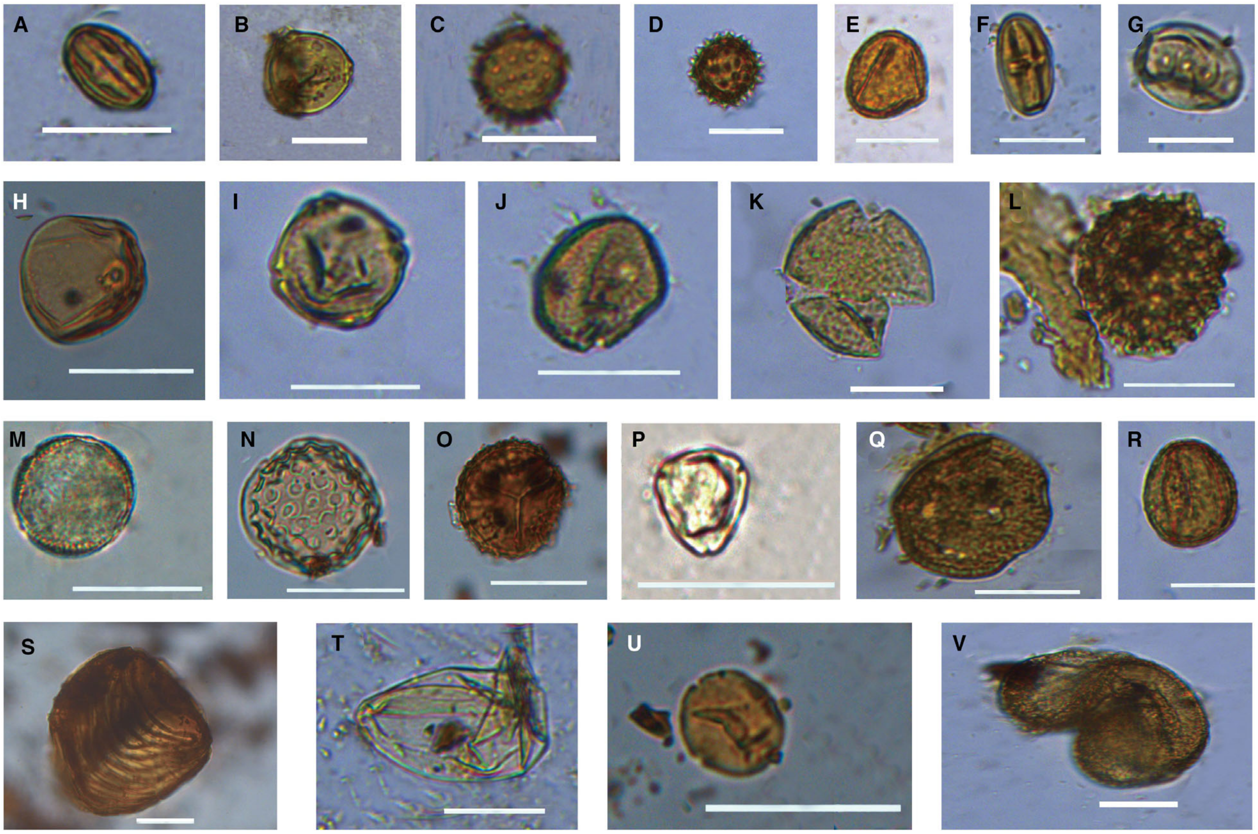

Fig. 5. Main pollen morphotypes found at the Wanbei site. A. *Castanopsis*. B. Carpinus. C. Chenpodiaceae. D. Compositae. E. *Cyclobalanopsis*. F. Umbelliferae. G. Juglandaceae. H. Poaceae. I. Myriophyllum. J. Typha. K. Labiatae. L. Polygonaceae. M. *Artemisia*. N. Zygnemataceae. O. Lycopodiaceae. P. Myrtaceae. Q. Caryophyllaceae. R. *Quercus*. S. Ceratopteris. T. *Cyperaceae*. U. *Celtis*. V. *pinus*. Scale bar: 20 µm.

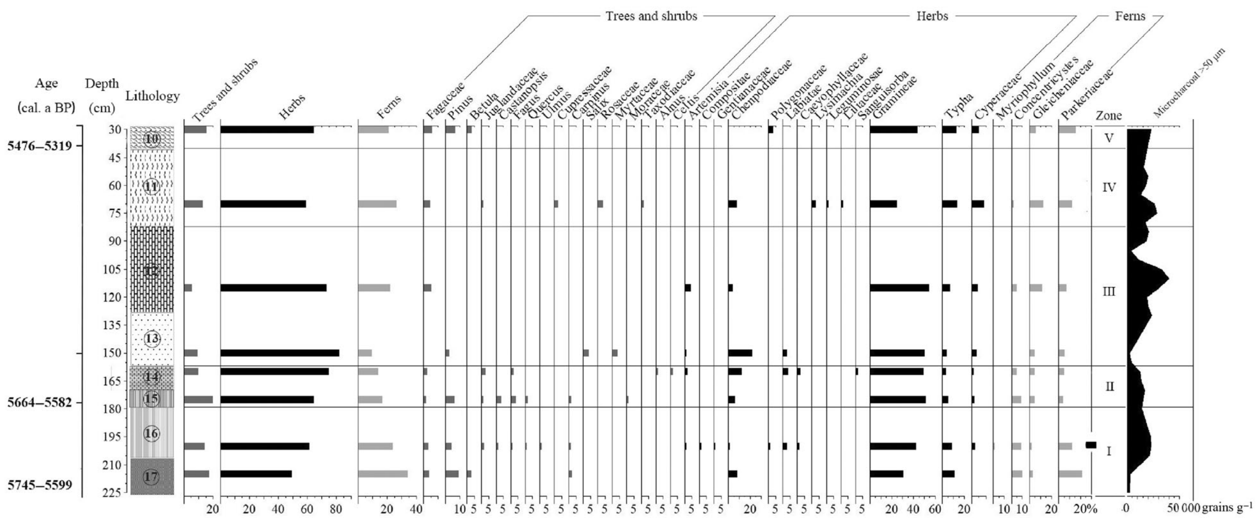

Fig. 6. Pollen percentage diagram and the microcharcoal concentrations for the sampled T1 at Wanbei site. Lithological details are provided in Table 1.

sum of herbaceous pollen is 77.3%, that of arboreal pollen is 7.1%, and that of fern spores is 15.6% (Fig. 6). The proportions of Poaceae pollen with a size ≥38 µm account for 63.8–64.7% of the total Poaceae pollen (Fig. 7). The mean concentration of coarse-grained microcharcoal increases to 20 483.87 grains g^{-1} (Fig. 7).

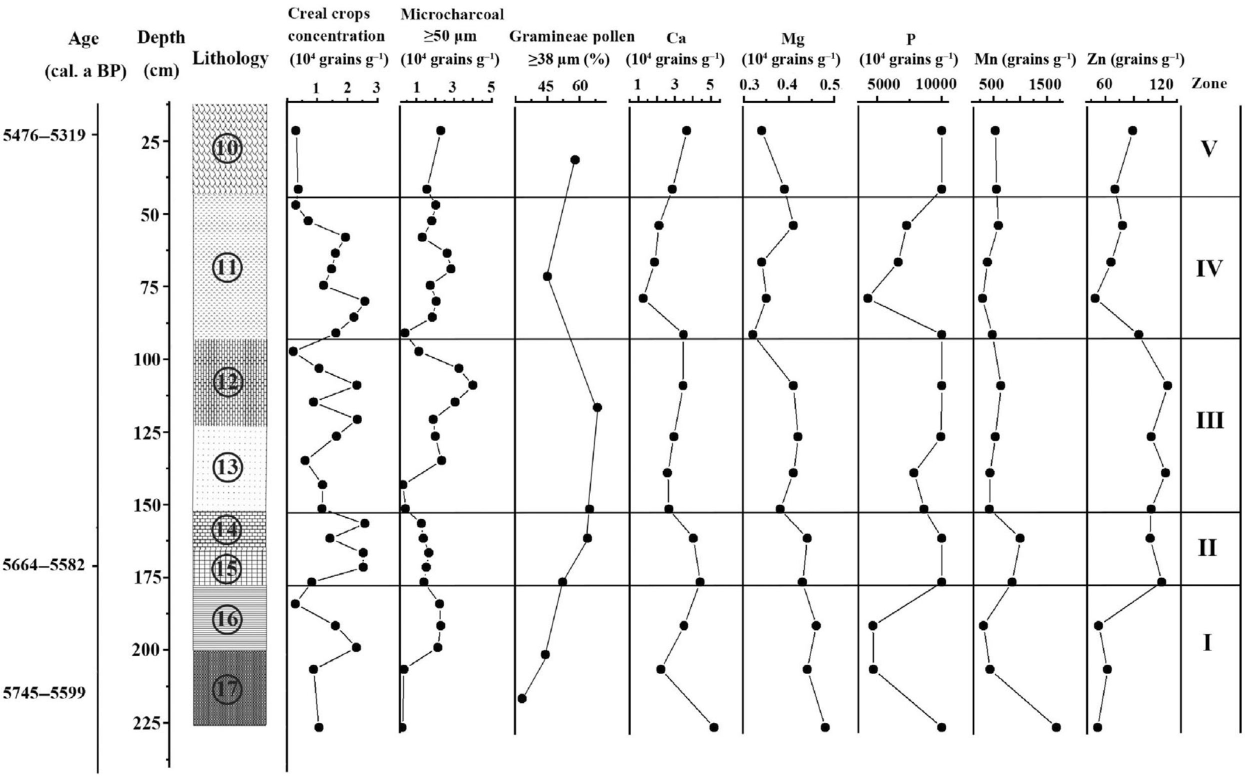

Fig. 7. Correlation of proxy records of human activities for the sampled T1 at Wanbei site. Lithological details are provided in Table 1.

In Zone IV, Poaceae pollen still occupies an important part of the assemblage, with a relative abundance of 24.27%. Arboreal pollen is characterized mainly by Fagaceae (4.27%). Hygrophyte pollen consists mainly of Cyperaceae (8.74%) and *Typha* (13.11%). The average total sum of herbaceous pollen is 58.7%, that of arboreal pollen is 12.6%, and that of fern spores is 26.2% (Fig. 6). The proportion of Poaceae pollen with a size ≥38 μm accounts for 45% of the total Poaceae pollen (Fig. 7). The mean concentration of coarse-grained microcharcoal is 18 595.65 grains g^{-1} (Fig. 7).

In Zone V, the pollen assemblages are still dominated by Poaceae pollen, with a relative abundance of 43.65%. Arboreal pollen is characterized primarily by *Pinus* (6.35%) and Fagaceae (5.56%). The average total sum of herbaceous pollen is 64.3%, that of arboreal pollen is 15.1% and that of fern spores is 20.63% (Fig. 6). The proportion of Poaceae pollen with a size ≥38 μm accounts for 58% of the total Poaceae pollen (Fig. 7). The mean concentration of coarse-grained microcharcoal is 19 289.05 grains g^{-1} (Fig. 7).

Chemical element analysis results

A total of 60 ultratrace and rare earth elements were detected within the soil samples collected from the Wanbei site. Previous studies have indicated that the variations in aluminium (Al), iron (Fe), lithium (Li) and scandium (Sc) in cultural layers are particularly responsive to the chemical weathering processes that are affected mainly by climate change and hence are good indicators of the Asian summer monsoon (Ma *et al.* 2006; Li *et al.* 2008). Alternatively, the variations in phosphorus (P), zinc (Zn), manganese (Mn), calcium (Ca) and magnesium (Mg) in the cultural layers are significantly correlated with the compositions of human settlements, animal remains and domestic waste (Li *et al.* 2008; Wilson *et al.* 2008). Therefore, these variables are biogeochemical markers reflecting the intensity and fluctuations of human activities over time.

In Zone I, the mean concentrations of Al, Li, Fe and Sc are 4.77×10^4, 22.5, 2.12×10^4 and 6.7 μg g^{-1}, respectively. Within the range of depths examined, the elemental concentrations remained relatively stable, with a slight decrease observed with increasing depth, as depicted in Fig. 8 The mean concentrations of P, Zn, Mn, Ca and Mg were 0.645×10^4, 55.7, 811, 3.64×10^4 and 0.46×10^4 μg g^{-1}, respectively. Their concentrations reach maximum values at a depth of 225 cm and then sharply decrease at a depth of 200 cm (Fig. 7).

In Zone II, the mean concentrations of Al, Li, Fe and Sc slightly decrease compared with those in Zone I, with the Al, Li, Fe and Sc concentrations of 4.34×10^4, 19.7, 1.83×10^4 and 5.9 μg g^{-1}, respectively (Fig. 8). However, the P, Zn, Mn, Ca and Mg distributions in this zone tend to increase compared with those in Zone I. The mean concentrations are 0.954×10^4, 113, 929, 4.22×10^4 and 0.435×10^4 μg g^{-1}, respectively, with the highest values occurring at a depth of 175 cm (Fig. 7).

In Zone III, the mean concentrations of Al, Li, Fe and Sc continue to decrease. The average concentrations decrease to 3.34×10^4, 14.5, 1.19×10^4 and 4.5 μg g^{-1}, respectively (Fig. 8). The P (0.91×10^4 μg g^{-1}), Zn (116 μg g^{-1}) and Mg (0.41×10^4 μg g^{-1}) concentrations are basically equal to those in the previous zone, although the Mn and Ca concentrations decrease to 510 and 2.95×10^4 μg g^{-1}, respectively (Fig. 7).

Compared with those in Zone III, the Al, Li, Fe and Sc contents in Zone IV tend to reverse. The mean values increase, reaching values of 4.51×10^4, 18, 1.52×10^4 and 6.3 μg g^{-1}, respectively, with peak values for Al, Fe and Sc found at 75 cm depth (Fig. 8). In contrast, the mean P, Zn, Mn, Ca and Mg concentrations decrease by 0.704×10^4, 72, 436, 2.18×10^4 and 0.36×10^4 μg g^{-1}, respectively, with the lowest peak values of P, Zn, Mn and Ca occurring at 75 cm depth (Fig. 7).

In Zone V, the mean concentrations of Al (4.33×10^4 μg g^{-1}), Li (17.4 μg g^{-1}), Fe (1.42×10^4 μg g^{-1}) and Sc (5.7 μg g^{-1}) slightly decrease again (Fig. 8), whereas the P, Zn, Mn, Ca and Mg concentrations increased to more than 1.0×10^4, 79.5, 540, 3.27×10^4 and 0.37×10^4 μg g^{-1}, respectively (Fig. 7).

Discussion

Most phytoliths from archaeological soil are derived from local plants. Hence, phytolith assemblages, e.g. *Iw*, from archaeological sediments can provide a more accurate assessment as to how the environment responds to climatic changes over time (Wallis 2001; Li *et al.* 2010). As shown in Fig. 6, the *Iw* values fluctuated at low levels between 5700 and 5300 a BP, which are consistent with the phytolith assemblage zones. The dominance of warm types in the Zone I phytolith assemblage suggests a warm climate during the 5700 a BP period. The average *Iw* values then decrease to 0.53 and 0.49, showing a cooling trend during the periods of 5600 and 5400 a BP, respectively. This overall trend towards cool conditions is supported by evidence of decreases in the mean values of Al, Li, Fe and Sc, which are related to chemical weathering processes (Fig. 8). In addition, the pollen assemblages in Zones II and III also show increases in herbaceous pollen but marked decreases in arboreal pollen and fern spores, indicating a cooling trend and a reduction in the area of water bodies in the region. After that, both the *Iw* values and Al, Li, Fe and Sc contents

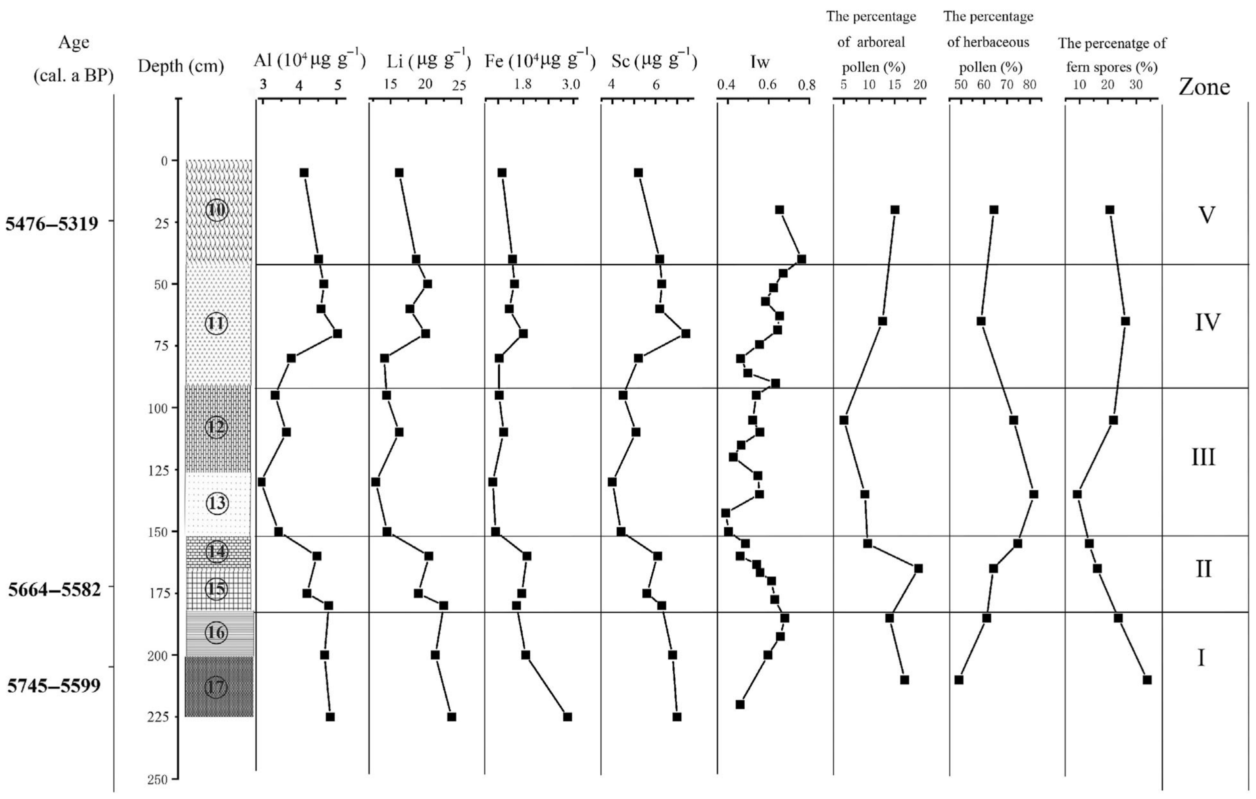

Fig. 8. Correlation of climatic proxy records of the samples T1 at Wanbei site. Lithological details are provided in Table 1.

increase, indicating that the climate became warm and humid again at Wanbei (Figs 3, 8). Multiple climate records assembled from the Huai River Basin and the surrounding region show that climatic conditions became warm and humid overall, with some fluctuations (Tang *et al*. 1993; Shu *et al*. 2009, 2012; Dong *et al*. 2013; Qin *et al*. 2015; Li *et al*. 2016; Qiu *et al*. 2020) after the onset of the Holocene optimum in the Huai River Basin (Jiang *et al*. 2018). Additionally, such a cooling event during the periods between 5600 and 5400 a BP was also recorded by several indicators derived from an archaeological soil succession at the Longqiuzhuang site (Zhu *et al*. 2000) and the natural drill cores in the nearby Taihu region (Yu *et al*. 2003; Qiu *et al*. 2020). These results confirm that the phytolith assemblages and chemical element variability in the archaeological sediment successions from the Wanbei site are indeed indicators of the response to local climatic conditions between 5700 and 5300 a BP.

The phytolith results at the Wanbei site indicate that rice was always the principal crop during the period of the Dawenkou culture (Figs 4, 8). In contrast, the contemporary Dawenkou cultural sites, e.g. the Dongpan and Beiqian sites on the side of the Mount Tai-Yi area, were characterized by millet-based farming strategies and had relatively dry environments (Jin *et al*. 2016). Rice is a typical thermophilic and hygrophilous plant that favours a warm and humid climate (Li 1983). Previous studies confirmed that the occurrence of rice cultivation was consistent with the initiation of the Holocene optimum in the Huai River Basin (Jiang *et al*. 2018). It is, therefore, believed that favourable water and thermal conditions facilitated rice agricultural activities at Wanbei between 5700 and 5300 a BP, while the emergence of millets is suggested to have resulted from the Dawenkou cultural exchange and from communication between the Haidai region in the north and the Huai River Valley (Cheng 2020; Tian *et al*. 2023).

Notably, however, the broomcorn millet percentages increased sharply from 3.14 to 14.26% and then reached 15.25%, whereas the rice proportions decreased from 96.86% to 85.56 and 84.48% in Zones I, II and III, respectively (Fig. 4). Moreover, the remains of foxtail millet appeared first in Zone II and then increased to 2.56% of the crop proportion in Zone III. After the cooling events during the periods of 5600 and 5400 a BP, the proportions of rice increased again, reaching 94.11 and 96.24%, respectively, whereas the proportions of foxtail millet and broomcorn millet were only 0.48 and 1.61% and 5.41 and 2.15%, respectively (Figs 4, 8). Both foxtail millet and broomcorn millet have strong cold and drought tolerances (Feng 2012). The adjustment of agricultural structures in response to climate change is a significant adaptation strategy to ensure agricultural sustainability and food safety. Hence, we believe that the significant increase in the proportion of millets was an adaptation strategy in response to the cooling event that occurred between 5600 and 5400 a BP at Wanbei. Archaeobotanical research also revealed that the status of rice cultivation declined in the Haidai region during the late Shang and early Zhou periods, with the rapid weakening of the East Asian summer monsoon at approximately 3000 a BP, although rice was one of the main crops cultivated during the Yueshi and Shang periods (Gong *et al*. 2019).

The distribution of a high proportion of Poaceae pollen with sizes ≥38 μm is directly related to agricultural activities (Wang *et al*. 2017). The data from Fig. 7 reveal a significant increase in the proportions of Poaceae pollen with sizes ≥38 μm from 30–44% to 52.17–63.8% and then to 63.8–64.7% from Zones I to II and III, suggesting that agricultural activities increased between 5600 and 5400 a BP at Wanbei. The total concentrations of crop phytoliths from Zones II and III were not lower or even higher than those from the previous period, also indicating that agricultural activities would have strengthened rather than weakened, although the rice concentrations were somewhat lower in Zone III. Alternatively, as shown in Fig. 7, the frequencies of the chemical elements that are affected mainly by human activities, e.g. P, Zn and Mn, increase significantly during the cooling period, when the concentration of coarse microcharcoal also peaks, although its frequency increases less significantly. The peak in the microcharcoal percentage, with high concentrations of P, Zn and Mn, combined with the results for the phytolith concentrations in cereal crops, suggests a cooling period when there was considerable exploitation of resources by early societies.

The cooling event, centered at 5.5 ka BP, corresponds with the orbitally induced lowering of Northern Hemisphere summer solar insolation (Wang *et al*. 2005), which is widely recorded in East Asian monsoon regions, e.g. stalagmite $\delta^{18}O$ measurements at Lianhua Cave (Zhang *et al*. 2013), Heshang Cave (Liu *et al*. 2020) and Sanbao Cave (Zhao *et al*. 2010), and the pollen record at Daihai Lake (Xiao *et al*. 2004), Qinghai Lake (Liu *et al*. 2002), Guxu Lake (Qiu *et al*. 2020) and others (Li *et al*. 2018). Cereal crops are very sensitive to variations in temperature and precipitation. Nevertheless, numerous studies indicate that agriculture at Yangshao cultural sites in the Central Plains region (Wang *et al*. 2017; Yang *et al*. 2024), Hongshan cultural sites in North China (Sun & Zhao 2013; Sun 2014), Youziling cultural sites in Jianghan plain (Yao *et al*. 2019; Yang *et al*. 2020), Dawenkou cultural sites in Haidai region (Jin *et al*. 2016; Guo 2019) and Longqiuzhuang site in the lower Huai River valley (Tang *et al*. 1996) made significant progress during the 5.5 ka BP period. According to Wu *et al*. (2018), the cooling event would impact the living and food production environment and the regional resource carrying capacity, and then trigger the population resource imbalance both in south and north China. Ancient people had to use sustainable agriculture practices, like manuring in north China (Yang *et al*. 2022), to achieve long-term productivity. Although no evidence of manuring practices has been revealed at Wanbei, and other contemporary sites in the middle and lower Huai River valley to date, the significant increase in numbers of late Dawenkou cultural sites here (Luan 2023; Wu *et al*. 2024) signifies the growth of population density, which should be facilitated by sustainable intensification in agriculture. It, therefore, has been suggested that the cooling event did not have a substantial negative impact on the development of agriculture in the aforementioned regions, in addition to the Wanbei site but promoted the simultaneous appearance of institutionalized socioeconomic inequalities in societies in multiple regions of China.

Conclusions

The data from multiple indicators presented in this paper indicate that the archaeological sediment successions from the Wanbei site record both significant natural and human-induced environmental changes. The climatic conditions at the Wanbei site were predominantly warm and humid between 5700 and 5300 a BP, whereas a cooling trend occurred during the period between 5600 and 5400 a BP. Rice has always been cultivated and domesticated as the main cereal crop in mixed farming owing to warm and humid conditions, although cooling events have facilitated an increase in the percentage of millets at Wanbei. Moreover, proxy records of human activities show that agricultural activities and the exploitation of resources by early societies were not weakened; in contrast, they showed a strengthening trend during the cooling period. This study not only highlights the dynamic nature of early agricultural societies and their adaptation to climatic changes at Wanbei but also enhances our understanding of human–climate interactions in the middle and lower Huai River valley during the Middle Holocene.

Acknowledgements. – This research was funded by the National Social Science Fund of China, grant number 22BKG044. We would like to thank the three reviewers of this study for their insightful comments and suggestions.

Author contributions. – WL and JZ conceived and designed the study. LL and HG provided the archaeological samples. WL and TS collected the study samples; WT and WL wrote the manuscript; WT and WL analysed the data; WT, WL, HX, YS, CZ and XW carried out the review and editing; WL and WT revised the paper; WL arranged funding acquisition. All authors have read and agreed to the published version of the manuscript.

Data availability statement. – The original data presented in the study are included in the article. Further inquiries can be directed to the corresponding authors.

References

Ball, T., Chandler-Ezell, K., Dickau, R., Duncan, N., Hart, T. C., Iriarte, J., Lentfer, C., Logan, A., Lu, H. & Madella, M. 2016: Phytoliths as a tool for investigations of agricultural origins and dispersals around the world. *Journal of Archaeological Science 68*, 32–45. https://doi.org/10.1016/j.jas.2015.08.010.

Burdanowitz, N., Gaye, B., Hilbig, L., Lahajnar, N., Lückge, A., Rixen, T. & Emeis, K.-C. 2019: Holocene monsoon and sea level-related changes of sedimentation in the northeastern Arabian Sea. *Deep Sea Research Part II: Topical Studies in Oceanography 166*, 6–18. https://doi.org/10.1016/j.dsr2.2019.03.003.

Chen, F. H., Dong, G. H., Zhang, D. J., Liu, X. Y., Jia, X., An, C.-B., Ma, M. M., Xie, Y. W., Barton, L., Ren, X., Zhao, Z. J., Wu, X. H. & Jones, M. K. 2015: Agriculture facilitated permanent human occupation of the Tibetan plateau after 3600 BP. *Science 347*, 248–250. https://doi.org/10.1126/science.1259172.

Cheng, Z. 2020: Primitive agriculture in Dawenkou culture period in Huai River valley of Anhui Province. *Agricultural Archaeology 1*, 22–28 (in Chinese).

Cheng, Z., Yang, Y., Gan, H., Lin, L. & Zhang, J. 2020: Analysis of carbonized plant remains in Wanbei site in Shuyang, Jiangsu Province in 2015. *Agricultural History of China 39*, 33–42 (in Chinese).

Cruz, P., Winkel, T., Ledru, M.-P., Bernard, C., Egan, N., Swingedouw, D. & Joffre, R. 2017: Rain-fed agriculture thrived despite climate degradation in the pre-Hispanic arid Andes. *Science Advances 3*, e1701740. https://doi.org/10.1126/sciadv.1701740.

Dearing, J. A., Battarbee, R., Dikau, R., Larocque, I. & Oldfield, F. 2006: Human–environment interactions: towards synthesis and simulation. *Regional Environmental Change 6*, 115–123. https://doi.org/10.1007/s10113-005-0012-7.

Dong, G., Jia, X., An, C., Chen, F., Zhao, Y., Tao, S. & Ma, M. 2012: Mid-Holocene climate change and its effect on prehistoric cultural evolution in eastern Qinghai Province, China. *Quaternary Research 77*, 23–30. https://doi.org/10.1016/j.yqres.2011.10.004.

Dong, G., Jia, X., Elston, R., Chen, F., Li, S., Wang, L., Cai, L. & An, C. 2013: Spatial and temporal variety of prehistoric human settlement and its influencing factors in the upper Yellow River valley, Qinghai Province, China. *Journal of Archaeological Science 40*, 2538–2546. https://doi.org/10.1016/j.jas.2012.10.002.

Faegri, K., Kaland, P. E. & Krzywinski, K. 1989: *Textbook of Pollen Analysis.* 328 pp. John Wiley and Sons, Chichester.

Feng, X. 2012: *Study on the difference of drought tolerance and physiological and ecological characteristics of different millet varieties.* M.Sc. thesis, Shanxi Normal University, unpaginated (in Chinese).

Ge, H., Chen, S., Wang, L., Wang, Z., Zhang, J. & Ge, M. 2008: Investigation and reflection on the comprehensive development and utilization of forest resources in Shuyang County. *Protection Forest Science and Technology 6*, 36–38 (in Chinese).

Gong, W., Fang, H., Guo, J. & Chen, X. 2019: Influence of climate change on rice agriculture in the late Shang dynasty – based on the observation of Shang dynasty plant remains in Daxinzhuang and Liujiazhuang sites in Jinan. *Quaternary Sciences 39*, 170–182 (in Chinese).

Grimm, E. C. 1987: CONISS: a FORTRAN 77 program for stratigraphically constrained cluster analysis by the method of incremental sum of squares. *Computers & Geosciences 13*, 13–35. https://doi.org/10.1016/0098-3004(87)90022-7.

Guo, R. 2019: *Archaeological study on prehistoric agriculture in Haidai area.* Ph.D. thesis, Shandong University, unpaginated (in Chinese).

Hu, F., Yang, Y. & Zhang, J. 2018: Environmental archaeological observation on the evolution of prehistoric human culture in the middle Huai River valley. *Southeast Culture 3*, 46–53 (in Chinese).

Huang, F. & Zhang, M. 2000: Pollen and phytolith evidence for rice cultivation during the Neolithic at Longqiuzhuang, eastern Jianghuai, China. *Vegetation History and Archaeobotany 9*, 161–168. https://doi.org/10.1007/BF01299800.

International Committee for Phytolith Taxonomy 2019: International code for phytolith nomenclature (ICPN) 2.0. *Annals of Botany 124*, 189–199. https://doi.org/10.1093/aob/mcz064.

Jia, M., Li, C., Mao, X., Zhang, D., Wei, C. & Liu, H. 2021: Climate–-human–environment interactions in the middle Yangtze Basin (central China) during the middle Holocene, based on pollen and geochemical records from the Sanfangwan site. *Catena 204*, 105357. https://doi.org/10.1016/j.catena.2021.105357.

Jiang, S., Luo, W., Tu, L., Yu, Y., Fang, F., Liu, X., Zhan, T., Fang, L., Zhang, X. & Zhou, X. 2018: The Holocene optimum (HO) and the response of human activity: a case study of the Huai River basin in eastern China. *Quaternary International 493*, 31–38. https://doi.org/10.1016/j.quaint.2018.08.011.

Jin, G., Wagner, M., Tarasov, P. E., Wang, F. & Liu, Y. 2016: Archaeobotanical records of Middle and Late Neolithic agriculture from Shandong Province, East China, and a major change in regional subsistence during the Dawenkou culture. *The Holocene 26*, 1605–1615. https://doi.org/10.1177/0959683616641746.

Jin, Q., Wang, P., Wang, S., Li, Z. & Zhang, G. 1987: The lower limit of the quaternary in the middle reaches of the Huai River plain in Anhui. *Marine Geology & Quaternary Geology 2*, 67–79 (in Chinese).

Kajita, H., Kawahata, H., Wang, K., Zheng, H., Yang, S., Ohkouchi, N., Utsunomiya, M., Zhou, B. & Zheng, B. 2018: Extraordinary cold episodes during the mid-Holocene in the Yangtze delta: interruption of the earliest rice cultivating civilization. *Quaternary Science Reviews 201*, 418–428. https://doi.org/10.1016/j.quascirev.2018.10.035.

Kawahata, H. 2019: Climatic reconstruction at the Sannai-Maruyama site between Bond events 4 and 3—implication for the collapse of the society at 4.2 ka event. *Progress in Earth and Planetary Science 6*, 1–18. https://doi.org/10.1186/s40645-019-0308-8.

Li, Z. 1983: Effect of temperature on rice growth and yield. *Hubei Agricultural Sciences 12*, 36–39 (in Chinese).

Li, M. 1991: Identification report on animal skeletons of Wanbei Neolithic site in Shuyang, Jiangsu Province. *Southeast Culture Z1*, 183–189 (in Chinese).

Li, R., Carter, J. A., Xie, S., Zou, S., Gu, Y., Zhu, J. & Xiong, B. 2010: Phytoliths and microcharcoal at Jinluojia archeological site in middle reaches of Yangtze River indicative of paleoclimate and human activity during the last 3000 years. *Journal of Archaeological Science 37*, 124–132. https://doi.org/10.1016/j.jas.2009.09.022.

Li, J., Dodson, J., Yan, H., Wang, W., Innes, J. B., Zong, Y., Zhang, X., Xu, Q., Ni, J. & Lu, F. 2018: Quantitative Holocene climatic reconstructions for the lower Yangtze region of China. *Climate Dynamics 50*, 1101–1113. https://doi.org/10.1007/s00382-017-3664-3.

Li, K., Gu, Y. & Liu, H. 2016: Holocene climate changes derived from spore-pollen records and Neolithic culture succession in northern Henan plain. *Journal of Jilin University (Earth Science Edition) 46*, 1449–1457 (in Chinese).

Li, C., Zheng, Y., Yu, S., Li, Y. & Shen, H. 2012: Understanding the ecological background of rice agriculture on the Ningshao Plain during the Neolithic Age: pollen evidence from a buried paddy field at the Tianluoshan cultural site. *Quaternary Science Reviews 35*, 131–138. https://doi.org/10.1016/j.quascirev.2012.01.007.

Li, Z., Zhu, C., Zhang, G., Ouyang, J. & Wang, R. 2008: Study on the relationship between environmental changes recorded in Liaowadian site in Hubei Province and human activities. *Quaternary Sciences 28*, 1145–1159 (in Chinese).

Liu, X., Liu, J., Chen, S., Chen, J., Zhang, X., Yan, J. & Chen, F. 2020: New insights on Chinese cave δ^{18}O records and their paleoclimatic significance. *Earth-Science Reviews 207*, 103216. https://doi.org/10.1016/j.earscirev.2020.103216.

Liu, X., Shen, J., Wang, S., Yang, X., Tong, G. & Zhang, E. 2002: A 16000-year pollen record of Qinghai Lake and its paleo-climate and paleoenvironment. *Chinese Science Bulletin 47*, 1931–1936. https://doi.org/10.1360/02tb9421 (in Chinese).

Lu, H., Zhang, J., Wu, N., Liu, K., Xu, D. & Li, Q. 2009: Phytoliths analysis for the discrimination of foxtail millet (*Setaria italica*) and common millet (*Panicum miliaceum*). *PLoS One 4*, e4448. https://doi.org/10.1371/journal.pone.0004448.

Luan, F. 2023: On adult male and female graves in Dawenkou culture period. *East Asia Archaeology 1*, 15–27 (in Chinese).

Luo, W., Gu, C., Yang, Y., Zhang, D., Liang, Z., Li, J., Huang, C. & Zhang, J. 2019: Phytoliths reveal the earliest interplay of rice and broomcorn millet at the site of Shuangdun (ca. 7.3–6.8 ka BP) in the middle Huai River valley, China. *Journal of Archaeological Science 102*, 26–34. https://doi.org/10.1016/j.jas.2018.12.004.

Luo, W., Zhang, J., Yang, Y., Yin, C., Lin, L. & Gan, H. 2021: Analysis of phytolith in Shunshanji site in Sihong, Jiangsu Province and its environmental significance. *Acta Micropalaeontologica Sinica 38*, 3 (in Chinese).

Ma, C. M., Zhu, C., Zhu, G., Wang, J., Huang, R. & Gu, W. 2006: Study on magnetic susceptibility and element geochemical Records of Yuchisi Site in Mengcheng, Anhui Province. *Journal of Stratigraphy 30*, 124–130 (in Chinese).

MacDonald, G. M., Larsen, C. P., Szeicz, J. M. & Moser, K. A. 1991: The reconstruction of boreal forest fire history from lake sediments: a comparison of charcoal, pollen, sedimentological, and geochemical indices. *Quaternary Science Reviews 10*, 53–71. https://doi.org/10.1016/0277-3791(91)90030-X.

Murari, K. K., Jayaraman, T. & Swaminathan, M. 2018: Climate change and agricultural suicides in India. *Proceedings of the National Academy of Sciences of the United States of America 115*, E115. https://doi.org/10.1073/pnas.1714747115.

Nanjing Museum 1992: Brief report on excavation of Neolithic remains at Wanbei site in Shuyang, Jiangsu Province. *Southeast Culture 1*, 124–133 (in Chinese).

Park, J., Yi, S., Cheul Kim, J., Lee, E. & Choi, J. 2019: Abrupt Holocene climate shifts in coastal East Asia, including the 8.2 ka, 4.2 ka, and 2.8 ka BP events, and societal responses on the Korean peninsula. *Scientific Reports 9*, 10806. https://doi.org/10.1038/s41598-019-47264-8.

Perşoiu, A., Ionita, M. & Weiss, H. 2019: Atmospheric blocking induced by the strengthened Siberian high led to drying in west Asia during the 4.2 ka BP event – a hypothesis. *Climate of the Past 15*, 781–793. https://doi.org/10.5194/cp-15-781-2019.

Piperno, D. R. 2014: *Phytolyth Analysis: An Archaeological and Geological Perspective.* 1639 pp. Elsevier, Amsterdam.

Pleskot, K., Apolinarska, K., Kołaczek, P., Suchora, M., Fojutowski, M., Joniak, T., Kotrys, B., Kramkowski, M., Słowiński, M., Woźniak, M. & Lamentowicz, M. 2020: Searching for the 4.2 ka climate event at Lake Spore, Poland. *Catena 191*, 104565. https://doi.org/10.1016/j.catena.2020.104565.

Qin, X., Zhang, L. & Mu, Y. 2015: Holocene climate change in the semi-humid area of Huai River valley in the transitional zone between north and south in eastern China. *Quaternary Sciences 35*, 1509–1524 (in Chinese).

Qiu, Z., Jiang, H., Ding, J., Hu, Y. & Shang, X. 2014: Pollen and phytolith evidence for rice cultivation and vegetation change during the mid-late Holocene at the Jiangli site, Suzhou, East China. *PLoS One 9*, e86816. https://doi.org/10.1371/journal.pone.0086816.

Qiu, Z., Jiang, H., Ding, L. & Shang, X. 2020: Late Pleistocene-Holocene vegetation history and anthropogenic activities deduced from pollen spectra and archaeological data at Guxu Lake, eastern China. *Scientific Reports 10*, 1–14. https://doi.org/10.1038/s41598-020-65834-z.

Ran, M. & Chen, L. 2019: The 4.2 ka BP climatic event and its cultural responses. *Quaternary International 521*, 158–167. https://doi.org/10.1016/j.quaint.2019.05.030.

Shu, Q., Chen, Y., Zhang, M.-H. & Zhao, Z.-J. 2012: Environmental significance and clay mineral characteristics of YZ 1 core sediments in Zhouzhuang, northern Jiangsu plain. *Scientia Geographica Sinica/Dili Kexue 32*, 168–188 (in Chinese).

Shu, Q., Li, C. & Zhao, Z. 2009: The records of mass susceptibility and grain size for climate changes in Subei Basin during the last deglaciation. *Acta Sedimentologica Sinica 27*, 111–117 (in Chinese).

Shu, J., Wang, W., Jiang, L. & Takahara, H. 2010: Early Neolithic vegetation history, fire regime and human activity at Kuahuqiao, lower Yangtze River, East China: new and improved insight. *Quaternary International 227*, 10–21. https://doi.org/10.1016/j.quaint.2010.04.010.

Song, Z., Zheng, Y., Li, M., Zhang, Y., Wang, W., Wang, D., Zhao, C., Zhou, S., Zhu, Z. & Zhao, Y. 1999: *Fossil Spores and Pollen of China, Vol 1: The Late Cretaceous and Tertiary spores and pollen*. 207 pp. Science Press, Beijing (in Chinese).

Sun, Y. 2014: *Study on plant remains from Neolithic Age to Early Bronze Age in the upper reaches of West Liaohe River*. M.Sc. thesis, Inner Mongolia Normal University, unpaginated (in Chinese).

Sun, Y. & Zhao, Z. 2013: Comprehensive study on plant remains unearthed from Weijiawopu Hongshan culture site. *Agricultural Archaeology 33*, 1–5 (in Chinese).

Sun, W., Wang, B., Zhang, Q., Chen, D., Lu, G. & Liu, J. 2021: Middle East climate response to the Saharan vegetation collapse during the mid-Holocene. *Journal of Climate 34*, 229–242. https://doi.org/10.1175/JCLI-D-20-0317.1.

Tang, L., Li, M. & Sheng, C. 1991: Pollen identification report of Wanbei site in Shuyang, Jiangsu Province. *Southeast Culture Z1*, 190–192 (in Chinese).

Tang, L., Sheng, C., Zhao, X., Xiao, J., Yu, G. & Han, H. 1993: Vegetation and climate in Qingfeng section of Jianhu, Jiangsu Province in the past 10 thousand years. *Science China: B 23*, 637–643 (in Chinese).

Tang, L., Sun, J., Zhang, M. & Li, M. 1996: Primitive rice cultivation in Longqiuzhuang site, Gaoyou. *Acta Agronomica Sinica 22*, 608–612 (in Chinese).

Tian, W., Luo, W., Yang, Y., Gan, H., Cheng, Z., Sun, Y., Zhang, D., Lin, L. & Zhang, J. 2023: Multicropping pattern reveals human adaptation at the Wanbei site (ca. 5.7–4.4 ka cal. BP) in the Middle and Lower Huai River Valley, China. *Land 12*, 1158. https://doi.org/10.3390/land12061158.

Wallis, L. A. 2001: Environmental history of northwest Australia based on phytolith analysis at Carpenter's gap 1. *Quaternary International 83*, 103–117. https://doi.org/10.1016/S1040-6182(01)00033-7.

Wang, Y. & Lu, H. 1993: *The Study of Phytolith and its Application*. 278 pp. Ocean Press, Beijing (in Chinese).

Wang, Y., Cheng, H., Edwards, R. L., He, Y., Kong, X., An, Z., Wu, J., Kelly, M. J., Dykoski, C. A. & Li, X. 2005: The Holocene Asian monsoon: links to solar changes and North Atlantic climate. *Science 308*, 854–857. https://doi.org/10.1126/science.1106296.

Wang, F., Chien, N., Zhang, Y. & Yang, H. 1996: Pollen Flora of China. *Aerobiologia 2*, 153 pp.

Wang, W., Liu, J. & Zhou, X. 2003: Study on climatic index of phytolith deposited in Nanjing Homo erectus cave. *Chinese Science Bulletin 48*, 1205–1208 (in Chinese).

Wang, X., Mo, D., Li, C., Yu, S.-Y., Xue, B., Liu, B., Wang, H. & Shi, C. 2017: Environmental changes and human activities at a fortified site of the Liangzhu culture in eastern China: evidence from pollen and charcoal records. *Quaternary International 438*, 189–197. https://doi.org/10.1016/j.quaint.2017.05.001.

Wilson, C. A., Davidson, D. A. & Cresser, M. S. 2008: Multi-element soil analysis: an assessment of its potential as an aid to archaeological interpretation. *Journal of Archaeological Science 35*, 412–424. https://doi.org/10.1016/j.jas.2007.04.006.

Wu, W., Lin, L., Gan, H. & Jin, G. 2017: Phytolith evidence of settlement environment and industry in the second phase of Shunshanji, Sihong. *Agricultural History of China 36*, 3–14 (in Chinese).

Wu, X., Zhang, X., Yan, X., Zhang, X., Zhu, X. & Gan, H. 2024: Study on population migration in the late Dawenkou culture in the middle reaches of Huaihe River. *Jianghan Archaeology 4*, 124–132 (in Chinese).

Wu, W., Zheng, H., Hou, M. & Ge, Q. 2018: The 5.5 cal ka BP climate event, population growth, circumscription and the emergence of the earliest complex societies in China. *Science China Earth Sciences 61*, 134–148. https://doi.org/10.1007/s11430-017-9157-1.

Xiao, J., Xu, Q., Nakamura, T., Yang, X., Liang, W. & Inouchi, Y. 2004: Holocene vegetation variation in the Daihai Lake region of north-central China: a direct indication of the Asian monsoon climatic history. *Quaternary Science Reviews 23*, 1669–1679. https://doi.org/10.1016/j.quascirev.2004.01.005.

Xiao, J., Xu, S., Xiao, X., Tang, H., Chen, S., Han, Y., Gao, Y. & Qi, G. 2011: Analysis of phytolith in Guojiashan site in Nanjing and the cultural and environmental background of lake maturity. *Acta Palaeontologica Sinica 50*, 268–274 (in Chinese).

Xu, L. 2009: *The rise and fall of civilization: an ecological geological study on the ancient cultural layer of Weichi Temple Site in Mengcheng*. Ph.D. thesis, University of Science and Technology of China, unpaginated (in Chinese).

Yang, Y., Huang, C., Yao, L., Luo, W., Tao, Y., Luo, Y. & Zhang, D. 2020: Phytolith evidence of prehistoric agricultural development in Qujialing site, Jingmen, Hubei Province. *Quaternary Sciences 40*, 462–471 (in Chinese).

Yang, J., Yang, X., You, T. & Chen, F. 2024: The δ^{15}N values of foxtail millet (Setaria italica) and common millet (*Panicum miliaceum*) are reliable indicators of manuring practices. *Science China Earth Sciences 67*, 2910–2923. https://doi.org/10.1007/s11430-023-1376-y.

Yang, J., Zhang, D., Yang, X., Wang, W., Perry, L., Fuller, D. Q., Li, H., Wang, J., Ren, L. & Xia, H. 2022: Sustainable intensification of millet–pig agriculture in Neolithic North China. *Nature Sustainability 5*, 780–786. https://doi.org/10.1038/s41893-022-00905-9.

Yao, L., Tao, Y., Zhang, D., Luo, Y., Chen, Z., Luo, W., Yang, Y. & Tang, L. 2019: Analysis of carbonized plant remains in Qujialing site in Jingmen, Hubei Province. *Jianghan Archaeology 10*, 116–124 (in Chinese).

Yu, Y., Wu, H., Zhang, W., Boivin, N., Yu, J., Zhang, J., Zhou, X., Luo, W., Deng, C. & Ge, J. 2024: Climate and cultural evolution drove Holocene cropland change in the Huai River valley, China. *iScience 27*, 110841. https://doi.org/10.1016/j.isci.2024.110841.

Yu, S., Zhu, C. & Wang, F. 2003: Radiocarbon constraints on the Holocene flood deposits of the Ning-Zhen Mountains, lower Yangtze River area of China. *Journal of Quaternary Science 18*, 521–525. https://doi.org/10.1002/jqs.767.

Zapolska, A., Serge, M. A., Mazier, F., Quiquet, A., Renssen, H., Vrac, M., Fyfe, R. & Roche, D. M. 2023: More than agriculture: analysing time-cumulative human impact on European land-cover of second half of the Holocene. *Quaternary Science Reviews 314*, 108227. https://doi.org/10.1016/j.quascirev.2023.108227.

Zhang, X. 2018: *Study on the Neolithic cultural pattern in Huai River Valley*. Ph.D. thesis, Shandong University, unpaginated (in Chinese).

Zhang, J., Lu, H., Liu, M., Diao, X., Shao, K. & Wu, N. 2018: Phytolith analysis for differentiating between broomcorn millet (*Panicum miliaceum*) and its weed/feral type (*Panicum ruderale*). *Scientific Reports 8*, 13022. https://doi.org/10.1038/s41598-018-31467-6.

Zhang, H.-L., Yu, K.-F., Zhao, J.-X., Feng, Y.-X., Lin, Y.-S., Zhou, W. & Liu, G.-H. 2013: East Asian summer monsoon variations in the past 12.5 ka: high-resolution δ^{18}O record from a precisely dated aragonite stalagmite in central China. *Journal of Asian Earth Sciences 73*, 162–175. https://doi.org/10.1016/j.jseaes.2013.04.015.

Zhang, G., Zhu, C., Wang, J., Zhu, G., Ma, C., Zheng, C., Zhao, L., Li, Z., Li, L. & Jin, A. 2010: Environmental archaeology on Longshan culture (4500–4000 aBP) at Yuhuicun Site in Bengbu, Anhui Province. *Journal of Geographical Sciences 20*, 455–468. https://doi.org/10.1007/s11442-010-0455-8.

Zhao, K., Wang, Y., Edwards, R. L., Cheng, H. & Liu, D. 2010: High-resolution stalagmite δ^{18}O records of Asian monsoon changes in central and southern China spanning the MIS 3/2 transition. *Earth and Planetary Science Letters 298*, 191–198. https://doi.org/10.1016/j.epsl.2010.07.041.

Zhou, C. 1999: The foundation of the formation and development of prehistoric culture in Huaihe River basin – discussion on the primitive economy in Huai River valley. *Journal of Anhui University: Philosophy and Social Sciences Edition 5*, 8–14 (in Chinese).

Zhu, C., Zhao, N., Zhang, Q., Zhang, Y., Zhang, M. & Wu, J. 2000: Environmental archaeological research on the Neolithic site in Longqiuzhuang, Jiangsu Province. *Journal of Nanjing University: Natural Sciences 36*, 286–292 (in Chinese).